

Robustness of single-isocenter multiple-metastasis stereotactic radiosurgery end-to-end testing across institutions

Daniel L Saenz (✉ saenzdl@uthscsa.edu)

University of Texas Health Science Center at San Antonio <https://orcid.org/0000-0002-9372-992X>

Niko Papanikolaou

University of Texas Health Science Center at San Antonio

Emmanouil Zoros

National and Kapodistrian University of Athens

Evangelos Pappas

University of West Attica

Michael Reiner

Ludwig-Maximilians-Universitat Munchen

Lip Teck Chew

Farrer Park

Hooi Yin Lim

Farrer Park

Sam Hancock

Southeast Health

Alex Nevelsky

Rambam Health Care Campus

Christopher Njeh

Franciscan Health Inc

Georgios Anagnostopoulos

German Oncology Center

Research

Keywords: high definition dynamic radiosurgery (HDRS), intracranial brain metastases

Posted Date: March 4th, 2020

DOI: <https://doi.org/10.21203/rs.3.rs-15983/v1>

License:  This work is licensed under a Creative Commons Attribution 4.0 International License.

[Read Full License](#)

Abstract

Background The accuracy of stereotactic radiosurgery to multiple brain metastases with a single isocenter using high definition dynamic radiosurgery (HDRS) was evaluated to assess robustness, repeatability, and possibility of inter-institutional quality assurance amongst multiple institutions. **Methods** A CT simulation scan obtained from a previously treated patient was used as the data set for targeting seven brain lesions. A VMAT treatment plan was generated using Monaco and was replicated at six HDRS-capable institutions using a plan template. All institutions subsequently irradiated 3D-printed head anthropomorphic phantoms mimicking the patient's anatomy. Three different phantoms with a point dosimeter insert, film insert, and a gel dosimeter were used. Absolute dosimetry end-to-end dosimetric accuracy as well as gamma analysis for relative dose distribution agreement analysis was used to evaluate measurement agreement with calculation. **Results** Point measurements averaged across all institutions using six-degree-of-freedom treatment positioning correction were within $1.2 \pm 0.5\%$. The average gamma passing rate in the film plane using 3D global 3D gamma analysis was $96.6 \pm 2.2\%$ (3%/2 mm). For all targets within 4 cm of the isocenter, the 3D dosimetric gel gamma passing rate averaged across institutions was $>90\%$ (3%/2 mm). 88.0% average gamma passing rate was found for targets beyond 4 cm. The targeting accuracy of high definition dynamic radiosurgery assessed by geometrical offset of the center of dose distributions was established across multiple institutions in this study to be within 1 mm for targets within 4 cm of isocenter. **Conclusions** Across variations in clinical practice, comparable dosimetry and localization is possible with this treatment planning and delivery technique.

Background

For the treatment of intracranial brain metastases, the accuracy and efficiency of stereotactic radiosurgery (SRS) to treat multiple targets concurrently has been previously described in the literature¹⁻⁵. Specifically, the ability of Elekta Versa HD™ (Stockholm, Sweden) equipped with the Agility™ MLC, HexaPOD™ evo RT six-degree-of-freedom tabletop and in conjunction with the Monaco® treatment planning system (TPS) was investigated in this study at multiple institutions to show reproducible accuracy across variations in practice. The combined use of these technologies with cone-beam CT image guidance and six-degree-of-freedom couch patient positioning (enabled by XVI and HexaPOD) is termed by Elekta as high definition dynamic radiosurgery (HDRS). HDRS is characterized by the integration of optimization, planning, imaging and dose delivery techniques. Details of this technique and its accuracy were previously published in 2018⁶. The Monte Carlo-based TPS takes advantage of Agility MLC capabilities to effectively reduce the 5 mm leaf width in the jaw direction by positioning the Y-jaws within leaf widths on either end of the target(s). Since stereotactic targets may only require a few open leaf pairs, this jaw positioning accuracy can significantly improve target conformality. Treating off of the central-axis requires continuously travelling MLCs to track the targets as the gantry rotates, which is accomplished by MLCs travelling up to 6.5 cm/sec.

High geometric and dosimetric certainty is required for radiosurgery, and uncertainties arise from many sources. Hence, end-to-end tests are critical to examine the localization and dosimetric accuracy of the

entire process⁷. Our previous work described how HDRS dose distributions were validated at our institution with a patient-specific phantom, tailored to a particular patient's anatomy and filled with a dosimetric gel, in conjunction with similar phantoms equipped with point dosimeter and film inserts. However, such a technique is subject to differences in clinical practice between institutions due to variations in simulation technique, treatment planning strategy, alignment process and other factors. It was deemed important to conduct this standard protocol at several institutions in order to demonstrate the robustness of HDRS when subject to repeating the process between institutions.

This validation project was designed at the Mays Cancer Center at UT Health San Antonio as described in the previous publication. Other institutions included in the study are Ludwig Maximilian University of Munich (Munich, Germany), Farrer Park Hospital (Farrer Park, Singapore), Southeast Health (Cape Girardeau, Missouri, USA), Rambam Institution (Haifa, Israel), Franciscan Health (Indianapolis, Indiana, USA) and the German Oncology Center (Limassol, Cyprus). All institutions utilized the Elekta Agility collimator HDRS linear accelerator (Versa HD or Infinity) in conjunction with the Monaco treatment planning system. Results from all institutions were pooled and analyzed together for assessment with the exception of one site which did not have a HexaPOD six-degree-of-freedom tabletop, which is crucial for the overall accuracy of radiosurgery⁸. Hence, results for HDRS are best described by the six institutions with this capability.

Methods

Treatment Planning Dataset

An existing RT structure set from a previously-treated radiosurgery patient was chosen for the purpose of this study. The six metastatic lesions were modified in size in the CT data set ($0.74 \times 0.74 \times 1.25$ mm voxels) so that a range of targets with diameters from 6–25 mm could be treated. Target locations included lesions sufficiently far apart to measure up to 5.6 cm from isocenter to test the effects of rotational uncertainties on localization accuracy across the brain. The locations of the targets are shown in Fig. 1. In addition, a larger target was included for dose normalization purposes.

Phantom Design

The endpoint of this study was to assess accurate localization and dosimetry in an anatomically realistic measurement. Therefore, it was crucial to perform 3D dosimetry, which is possible with a gel dosimeter. The RTsafe PseudoPatient™ gel phantom produced by RTsafe P.C., (Athens, Greece) was used in this study as has been described in the literature^{9–10}. This dosimeter was chosen because it is a 3D dosimeter that can be cast in nearly any form, allowing for measurement in a patient-specific geometry. A modified composition of VIPAR polymer gels was used constituting of a mixture of the monomer N-vinylpyrrolidone in 6% weight fraction (wf), the cross-linker N, N' - methylene-bisacrylamide in 4% wf, gelatine of type A in 5% wf, deionized water in 85% wf, and 7 mM THPC^{6,11–12}. The primary advantage of gel dosimetry in an anthropomorphic phantom is that, unlike other patient-specific QA, it does not rely on

a recalculation of the plan on a phantom nor on the process with which to reconstruct a 3D dose distribution. Rather, the measurement in this phantom can be directly compared with the patient's calculated dose distribution as was demonstrated by Makris et al¹³. Finally, for the most realistic execution of an end-to-end test, an anthropomorphic phantom is the best substitute to approximate the entire process.

For the purposes of this study, three phantoms were produced by RTsafe based on the actual CT data set bony anatomy and external contour of our reference patient. The first was filled with the aforementioned dosimetric gel so that 3D dose measurements could be obtained. In addition, the other two phantoms were modified to accommodate placement of the other detectors. One had an insert for a one of two point dosimeters: Standard Imaging (Middleton, WI, USA) Exradin A16 or A26 ionization chamber (inside diameters of 2.4 and 3.3 mm respectively with collecting volumes of 0.007 and 0.015 cm³ respectively) or PTW (Freiburg, Germany) microdiamond detector (sensitive volume of 0.004 mm³). The other was designed with a holder for a Gafchromic film (Ashland, Bridgewater, NJ, USA). The point dosimeter and film cassette were situated to coincide with the center of the larger dose normalization target. By making point dosimeter measurements in a larger target less sensitive to small field dosimetry complications, the absolute dose accuracy can be shown with the point and film dosimetry and relative dose distribution characterized by gel dosimetry.

A planning template for HDRS delivery was devised in the Monaco version 5.11.02 treatment planning system (Elekta, Stockholm, Sweden) at UT Health San Antonio. This template consists of a set of beam geometries, prescription, and optimization objectives to be used across all institutions. The isocenter was set at the centroid of the targets. Five non-coplanar VMAT arcs were set up in the template (right and left lateral arcs with table at nominal 0°, right and left lateral oblique arcs with the table at 315° and 45°, and a vertex arc). As the dose linearity of the gel dosimeter breaks down above 12 Gy, the targets were assigned a prescription dose of 8 Gy with maximum doses remaining under 12 Gy. In all metastases, the dose was allowed to peak up to 12 Gy, while a homogeneous dose of 8 Gy was planned in the dose normalization target. No normal tissue objectives were defined and instead conformality at 8 Gy and 4 Gy was pursued. Target penalty, quadratic overdose and conformality objectives were used for optimization. A 1 mm dose calculation grid spacing was used with 1% statistical uncertainty per calculation of dose to medium. In the five single arcs, 180 control points were allowed with 0.5 cm minimum segment width. Medium fluence smoothing was used. For the multi-institutional study, the CT data set, RT structures and Monaco planning template, as well as the phantoms encompassing the point dosimeter and the Gafchromic cassette insert, were shared between all institutions in the study for the purposes of consistency of application. Upon receiving this data, institutions created their own treatment plans following the planning template.

Treatment Delivery

Patient data was sent to the Versa HD linear accelerator for delivery. The gel phantom was treated first and was localized with an XVI VolumeView™ cone-beam CT scan, which was fused with the reference CT

data set. An example image of the phantom set up for plan delivery is shown in Fig. 2. The grey value (T + R) (translation and rotation) algorithm in XVI was used with a clipbox placed such that the entire brain was covered. The correction reference was placed at the isocenter. 6D corrections were applied using the HexaPOD tabletop prior to delivery. The process was repeated for the point dosimeter and film measurements.

Film dosimetry and uncertainty

Gafchromic EBT3 film was used for the film phantom measurement. The $14 \times 8 \text{ cm}^2$ Gafchromic EBT3 films were calibrated at the Secondary Standard Dosimetry Lab of the Greek Atomic Energy Commission and follows AAPM Task Group 55 in water equivalent material¹⁴. Film was shipped to each institution and evaluated upon return providing dose maps in absolute Gy values. Since it can take varying durations for an institution to perform the irradiations, the time-dependent calibration curve was built using films scanned at 24 and 72 hours, as well as 5 and 8 days after irradiation. An EPSON (Seiko Epson Corp., Japan) V850 PRO flatbed scanner was used with 150 dpi digitization and 48-bit depth. More details are presented in our previous work on end-to-end accuracy at a single institution⁶.

The main source of the uncertainties involved in EBT3 film measurements is the calibration procedure and specifically the calibration curve fitting process¹⁵. An estimation of the range of the combined 1σ dosimetric uncertainties was performed by following the methodology described in Pappas et al. (2017)¹⁶ for triple channel film dosimetry since the calibration component is dose dependent¹⁵. Optical density measurement reproducibility, optical scanner homogeneity and film calibration, statistical and systematic dose uncertainties were included in the final estimation. A combined 1σ dosimetric uncertainty of 2.3% was estimated for the dose level of 8 Gy which was the prescription dose. According to Pappas et al. (2017)¹⁶ study, a spatial 1σ uncertainty of 1.5 mm is resulting from the spatial registration procedure between scanned film images and the CT dataset of the film phantom following a registration technique described elsewhere^{13,16}.

Dose extraction from Gel phantom

The gel phantoms were scanned on the MRI units of each institution one day after irradiation. Gel dose read-outs were performed using a variety of MRI units including, GE 1.5T Sigma HDX and 3T Optima 750 MW, Siemens 1.5T Espree and Sonata Vision and 3T Trio Tim, as well as Phillips 1.5T Ingenia. A 2D, multi-slice, multi-echo, Half Fourier Single Shot Turbo Spin Echo (HASTE) proton density to T2-weighted sequence was implemented sequentially using the head coil. Averaging was set to $n = 14$ to improve signal-to-noise ratio. MR-related geometric distortion was reduced with a bandwidth set to 1220 Hz/pixel. The MR protocol used is the one developed and recommended by the gel producer (RTsafe P.C.). Since the relaxation rate ($R2 = 1/T2$) of the polymer gel is directly proportional to absorbed dose, the MR scan was compared with the patient-derived planning CT data set for dose analysis. The acquired MR images were spatially co-registered with the corresponding CT datasets by performing bone-rigid registration using Monaco since the phantoms provide adequate bone and soft tissue signal in both CT and MR

images. Doses were normalized at each site to an appropriate ROI in the larger dose normalization PTV. 3D gamma analysis and dose profile comparisons were performed for analysis.

The linear relationship between measured R2 relaxation rates and delivered dose up to 12 Gy has been verified in previous studies for the same gel formulation used in this work^{11,17} and for a time window from 24 hours up to 15 days between gel irradiation and MRI scanning^{11,18}. The gel dose uncertainty component, regarding the duration between the gel fabrication and irradiation for a time interval of 6 days has been found less than 2%¹⁸. For the purposes of this study, only relative gel dose measurements were performed in order to avoid any potential sources of uncertainty that affect absolute gel dosimetry¹⁹. uncertainty level from the fitting procedure (linear fit) was calculated based on Papadakis et al (2007)¹² methodology. An estimation of the main sources of uncertainties for relative dose measurements was performed, revealing a dosimetric 1σ uncertainty less than 3%. Moreover, taking into account the spatial resolution of the MR images and the registration technique between MR gel data and CT dataset of the gel-filled phantom, a spatial 1σ uncertainty less than 2 mm.

Data analysis (phantom evaluation)

Point dosimeter measurements were evaluated by comparing to the average dose in a region of interest (ROI) indicating the position of a point dosimeter's sensitive volume in the plan calculation. Each institution followed standard dosimetry protocols in the conversion of measured charge to absorbed dose using k_q and other correction factors from a previous machine calibration. The point dosimetry measurement established the absolute dose levels for the gel dosimetry. Measured 2D and 3D doses were compared to the planned dose distribution after following a rigid image registration procedure using the film fiducials for the film analysis and using the cranial anatomy for the MRI scan. From this point, direct dose profile comparisons can be made. 3D gamma analysis for both the film and gel dosimeter was conducted by utilizing global gamma analysis with various passing criteria. Gamma analysis was performed in the film plane ROI and in the region of individual targets for the 3D gel analysis using the DICOM RTStruct file. In both dosimetric systems, the measured dose distribution was set as the reference one and the TPS calculated as the evaluated during gamma calculations applying a dose threshold of 20%. Finally, consortium-wide plots of sample dose profiles were evaluated and consortium-wide dose volume histograms (DVHs) were assessed to demonstrate the relative difference between the shapes of planned and delivered DVH.

Results

Point dosimeter measurements

Point measurements made in the dose normalization target agreed with TPS calculations (mean dose within a contour of the detector) The percentage difference between planned and measured dose was calculated (Table 1). A maximum percent difference of 1.7% was observed. The mean percent difference was 1.2% with a standard deviation of 0.5%.

Measured Versus Calculated Dose In Point Measurements

Table 1

In the dose normalization target, percent differences between measured dose and TPS calculated doses are shown at each institution.

Institution	% deviation
1	0.9%
2	1.7%
3	1.1%
4	1.3%
5	1.7%
6	0.3%
Average	1.2%

Film Analysis

3D Gamma analysis was used to analyze the measured dose distribution in the plane of the film insert. This means that the measured dose plane was compared with the 3D dose distribution from the treatment planning system, not just a planar dose. At 3%/2 mm and 2%/2 mm, the average and standard deviation of gamma passing rates were $96.9 \pm 2.1\%$ and $95.1 \pm 2.8\%$ respectively. A visual indication of the gamma results in the film plane is shown in Fig. 3 along with the tabulated results in Table 2.

Per Institution Film 3d Gamma Passing Rates

Table 2

Film gamma analysis passing rates at each institution in the film plane. Results are shown for two gamma criteria.

Institution	3%/2 mm gamma analysis passing rate ($\gamma < 1$)	2%/2 mm gamma analysis passing rate ($\gamma < 1$)
1	98.2%	96.9%
2	98.3%	96.5%
3	93.2%	89.4%
4	95.7%	94.2%
5	95.6%	94.8%
6	98.8%	96.6%
Average	96.6%	94.7%

Gel Phantom Analysis

For the 3D gel phantom analysis, gamma distributions within the targets were analyzed using the dose information from the T2 values and the planned 3D dose distribution. This was analyzed in conjunction with target diameter and distance from isocenter. Figure 4 shows example isodose lines from measurement and calculation in the indicated region of interest. At 3%/2 mm, the average gamma passing rate across institutions was $\geq 90\%$ for targets within 4 cm of isocenter. Two targets were beyond 4 cm of isocenter, for which an average gamma passing rate of 82.7% and 93.3% was measured. Table 3 summarizes this data.

Per Institution 3d Gel Gamma Passing Rates

Table 3

3D Gamma passing rate for each target (at the specified distance from isocenter) averaged across all institutions. Sample standard deviations are indicated.

Target	Target diameters (mm)	Distance from isocenter (cm)	Mean Gamma Passing Rate (%) (3%,2 mm)
T01	13	2.6	93.5 ± 7.1
T02	21	3.0	95.3 ± 3.7
T03	6	5.6	93.3 ± 6.7
T04	25	3.7	93.8 ± 2.0
T05	9	4.8	82.7 ± 16.3
T06	17	3.4	93.3 ± 5.6

Figure 4. (a) Axial CT image of the real patient with a region of interest. (b) Isodose lines (percentages relative to prescription dose) in the region of interest shown in (a).

An illustration of measured dose accuracy repeatability across institutions is shown in Fig. 5 where dose profiles for each site are plotted together. Figure 6 illustrates the physical positioning accuracies found for all targets and all institutions quantified by assessing the center-of-mass of the dose distribution in the measured and calculated 3D data and reporting the distance between them. It is plotted in the order of target volume as well. In this study, < 1 mm spatial accuracy for targets within 4 cm of isocenter was found. Beyond 4 cm, the highest spatial deviation recorded was 1.9 mm. Finally, a sample consortium-wide DVH measurement is shown in Fig. 7 normalized to D50 which exemplifies the degree to which the steepness of the planned DVH is degraded in the measurement.

Figure 5. (a) Axial CT image of the real patient. (b) 1D profile comparison between all consortium sites with HexaPOD of measured gel dose distributions (RTsafe) at the location depicted by the red line in (a). Error bars correspond to ± 1 mm spatial uncertainty.

Discussion

Agreement between HDRS measurement and TPS calculation was repeatable across institutions in this study where we are extending targeting accuracy from a point (conventional SRS) to an 8 cm diameter sphere. This was verified using 3D gamma analysis for both film and gel phantom measurements. Absolute dose verification within 2% is well within recommendations for SRS end-to-end dosimetric accuracy (5% per AAPM MPPG 9.a)⁷, demonstrating satisfactory results when compared with conventional SRS.

The advantages and critical need for the use of 6D corrections was re-affirmed by this study. The cross-consortium mean gamma passing rate for the targets beyond 4 cm was raised by 5.0% and 6.5% simply by excluding results from one site without HexaPOD rotational corrections. 6D corrections are essential for the end-to-end accuracy of a multiple-target SRS program since small rotational errors are of an increasing magnitude with increasing distance from isocenter and with decreasing target diameter. Even a 1-degree rotation can result in a 1 mm positioning error for a target 6 cm beyond isocenter. Particularly for small targets at this distance, rotational errors can result in substantial geometric miss unless rotational corrections are performed. Of note, rotational uncertainties arise from multiple sources (patient positioning, collimator angle, and couch angle when applying couch rotations without fiducials) and are all inherent in this study.

Rotational uncertainties remain a concern for a stereotactic delivery even with 6D corrections, although they are much smaller. When analyzing dose profiles across the targets, highly conformal profiles are evident in addition to areas of slight misalignment. While some slight localization error is expected, due not only to inherent uncertainties in the technique but also due to uncertainties in the gel phantom analysis, it remains prudent to understand the applicability and limitations of this technique. In regions distant to the isocenter, it would be wise to strategize carefully when applying this technique clinically. Typical SRS accuracy of < 1 mm breaks down beyond this region. Nevertheless, clinically acceptable plans can be created with applied setup margins with careful attention paid to cumulative metrics such as dose conformity and gradient index for all targets and total volumes of normal brain receiving a safe dose level. Alternatively, it may be wise to use separate isocenters to treat two groups of targets. While this may reduce the efficiency of the technique, it represents a compromise between efficiency of delivery and accuracy of dose delivery.

Being the first 3D end-to-end study of its kind (the first multi-center, multi-target accuracy study), the results of this study suggest the feasibility of establishing standards for HDRS accreditation or audits for newer institutions considering this technology. The quantitative results also can serve as a benchmark for assessing baseline accuracy and can aid in the commissioning process. Limitations of the study include need to use the same structures at each site. This was necessary in order to compare results across institutions but did limit the degree to which the study was a true end-to-end test at specific institutions. Furthermore, no verification imaging was conducted at couch angles other than the nominal angle. This could be resolved by use of in-room or gantry-mounted kV planar imaging²⁰ or potentially with surface imaging.

Conclusions

Precise stereotactic radiosurgery to multiple targets in the brain with a single isocenter has been demonstrated across multiple institutions to be a feasible approach. The combination of Monaco, Versa HD with HDRS, Agility and HexaPOD enables successful treatment of multiple brain metastases using a single isocenter SRS technique and the end-to-end accuracy results can be effectively measured with the use of the RTsafe PseudoPatient 3D gel phantom. The work presented here validates the results of a

single institution by showing comparable accuracy amongst institutions across the world. This study found submillimeter targeting accuracy at all institutions within an 8 cm diameter sphere around the treatment isocenter.

List Of Abbreviations

AAPM:	American Association of Physicists in Medicine
CT:	computed tomography
D50:	dose to 50% volume
DICOM:	Digital Imaging and Communications in Medicine
DVH:	dose-volume histogram
HASTE:	half Fourier single shot turbo spin echo
HDRS:	high definition dynamic radiosurgery
kV:	kilovoltage
MLC:	multi-leaf collimator
MPPG:	Medical Physics Practice Guidelines
MR:	magnetic resonance
MRI:	magnetic resonance imaging
PTV:	planning target volume
QA:	quality assurance
ROI:	region of interest
RT:	radiation therapy
RTStruct:	radiation therapy structure
SRS:	stereotactic radiosurgery
TPS:	treatment planning system
VIPAR:	N-vinyl pyrrolidone argon
VMAT:	volumetric modulated arc therapy

Declarations

Ethics approval and consent to participate

Not applicable due to no involvement of human participants.

Consent for publication

Not applicable.

Availability of data and materials

The datasets used and/or analyzed during the current study are available from the corresponding author on reasonable request.

Competing Interests

DS has received speaking fees for Elekta user's meetings.

NP is a stockholder with a less than 5% interest with RTsafe and a guest member of their Board of Directors.

EP and EZ also collaborate with the R&D department of RTsafe P.C.

RTsafe and Elekta have a collaboration framework.

Funding

This work was partially funded by a grant from Elekta to UT Health San Antonio.

Authors' Contributions

DS and NP designed the experimental protocol for planning and delivery. EZ and EP coordinated the gel dosimetry and analyzed all film and gel data. MR, LC, HL, SH, AN, CN, and GA all performed the delivery at their respective institutions. All authors contributed to the scientific conclusions in the paper.

Acknowledgements

Not applicable.

References

1. Clark GM, Popple RA, Edward Young P Fiveash JB. Feasibility of Single-Isocenter Volumetric Modulated Arc Radiosurgery for Treatment of Multiple Brain Metastases. *Intl J Rad Onc Biol Phys.* 2010;76(1): 296-302.

2. Pfeffer RM, Levin D, Spiegelmann R. Linac-based radiosurgery for multiple brain metastases: A quality assurance and feasibility study. *J Clin Onc.* 2017;35(15 sup): 2077.
3. Limon D, McSherry F, Herndon J, Sampson J, Pecci P, Adamson J, Wang Z, Yin FF, Floyd S, Kirkpatrick J, Kim GJ. Single fraction stereotactic radiosurgery for multiple brain metastases. *Adv Radiat Oncol.* 2017;2(4): 555-563.
4. Lau SKM, Zakeri K, Zhao X, Carmona R, Knipprath E, Simpson DR, Nath SK, Kim GY, Sanghvi P, Hattangadi-Gluth JA, Chen CC, Murphy KT. Single-Isocenter Frameless Volumetric Modulated Arc Radiosurgery For Multiple Intracranial Metastases. *Neurosurg.* 2016;77(2):233-240.
5. Huang Y, Chin K, Robbins JR, Kim J, Li H, Amro H, Chetty IJ, Gordon J, Ryu S. Radiosurgery of multiple brain metastases with single-isocenter dynamic conformal arcs (SIDCA). *Radiother Oncol.* 2014;112(1):128-132.
6. Saenz DL, Li Y, Rasmussen K, Stathakis S, Pappas E, Papanikolaou N. Dosimetric and localization accuracy of Elekta high definition dynamic radiosurgery. *Phys Medica.* 2018;54(2018): 146-151.
7. Halvorsen PH, Cirino E, Das IJ, Garrett JA, Yang J, Yin FF, Fairbrent LA. AAPM-RSS Medical Physics Practice Guideline 9.a. for SRS-SBRT. *Med Phys.* 2017;18(5): 10-21.
8. Dhabaan A, Schreibmann E, Siddigi A, Elder E, Fox T, Ogunleye T, Esiashvili N, Curran W, Crocker I, Shu HK. Six degrees of freedom CBCT-based positioning for intracranial targets treated with frameless stereotactic radiosurgery. *J Appl Clin Med Phys.* 2012; 13(6):3916.
9. Kalaitzakis G, Papanikolaou N, Boursianis T, Pappas EP, Lahanas V, Makris D, Stathakis S, Watts L, Efstathopoulos E, Maris TG, Pappas E. A quality assurance test for the validation of the spatial and dosimetric accuracy of a new technique for the treatment of multiple brain metastases. *Phys Medica.* 2016;32(3):327-328.
10. Maris TG, Pappas E, Boursianis T, Kalaitzakis G, Papanikolaou N, Watts L, Mazonakis M, Damilakis J. 3D polymer gel MRI dosimetry using a 2D haste, A 2D TSE AND A 2D SE multi echo (ME) T2 relaxometric sequences: Comparison of dosimetric results. *Phys Medica.* 2016;32(3):238-239.
11. Pappas, T. Maris, A. Angelopoulos, et al., A new polymer gel for magnetic resonance imaging (MRI). *Phys. Med. Biol.* 1999;44: 2677–2684.
12. E. Papadakis, T.G. Maris, F. Zacharopoulou, E. Pappas, G. Zacharakis, and J. Damilakis, An evaluation of the dosimetric performance characteristics of N-vinylpyrrolidone-based polymer gels. *Phys. Med. Biol.* 2007;52(16):5069–5083.
13. N. Makris, E.P. Pappas, E. Zoros, et al., Characterization of a novel 3D printed patient specific phantom for quality assurance in cranial stereotactic radiosurgery applications. *Phys. Med. Biol.* 2019;64(10):105009.
14. Niroomand-Rad A, Blackwell CR, Coursey BM, Gall KP, Galvin JM, McLaughlin WL, et al. Radiochromic Film Dosimetry Recommendations of AAPM Radiation Therapy Committee Task Group No. 55. *Med Phys.* 1998; 25(11): 2093-2115.
15. Aldelaijan, H. Mohammed, N. Tomic, et al., Radiochromic film dosimetry of HDR 192Ir source radiation fields. *Med. Phys.* 2011;38(11):6074–6083.

16. P. Pappas, E. Zoros, A. Moutsatsos, et al., On the experimental validation of model-based dose calculation algorithms for ^{192}Ir HDR brachytherapy treatment planning. *Phys. Med. Biol.* 2017;62(10):4160–4182.
17. Pappas, G. Kalaitzakis, T. Boursianis, et al., Dosimetric performance of the Elekta Unity MR-linac system: 2D and 3D dosimetry in anthropomorphic inhomogeneous geometry. *Phys. Med. Biol.* 2019;64(22):225009.
18. -V. Papoutsaki, T.G. Maris, E. Pappas, A.E. Papadakis, and J. Damilakis, Dosimetric characteristics of a new polymer gel and their dependence on post-preparation and post-irradiation time: Effect on X-ray beam profile measurements. *Phys. Medica.* 2013;29(5),453–460.
19. Baldock, Y. De Deene, S. Doran, et al., Polymer gel dosimetry, *Phys. Med. Biol.* 2010;55(5):R1–R63.
20. Yin FF, Wong J, Balter J, Benedict S, Bissonnette JP, Crain T, et al., The Role of In-Room kV X-Ray Imaging for Patient Setup and Target Localization: Report of Task Group 104 of the Therapy Imaging Committee American Association of Physicists in Medicine, 2009.

Figures

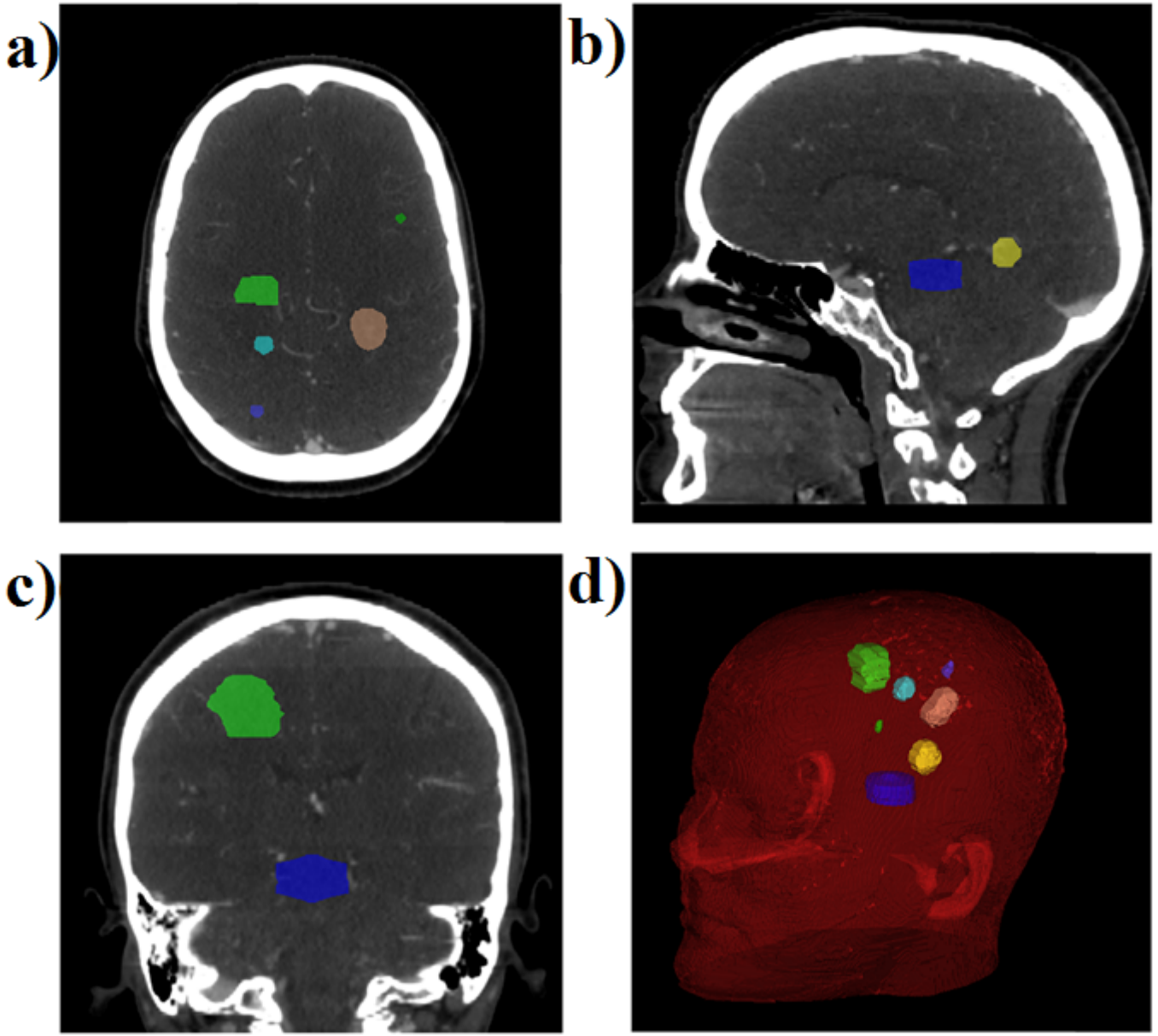


Figure 1

Location of the seven targets in the brain. a) axial, b) sagittal, and c) coronal sample slices are shown as well as (d) a three-dimensional model of the targets.

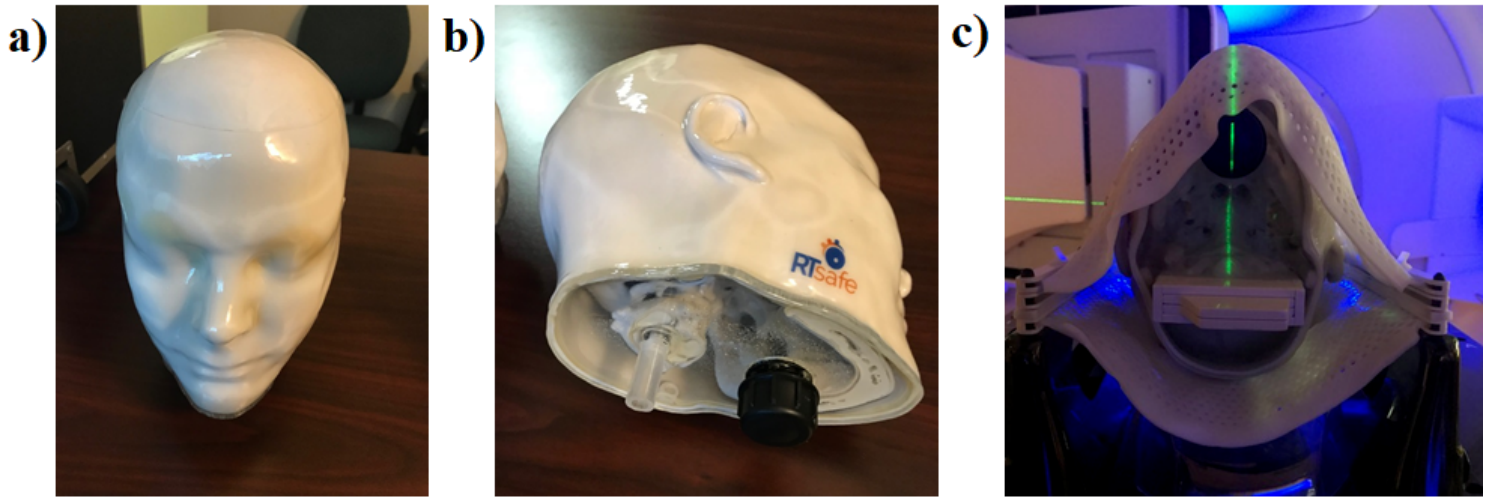


Figure 2

a) RTSafe PseudoPatient gel photograph b) Point dosimeter phantom photograph and c) Film phantom photograph of positioning for plan delivery.



Figure 3

3D gamma distribution (3%/2 mm) in the film plane across all six institutions using a HexaPOD table top. Film measured (red dashed lines) and TPS calculated (black solid lines) isodose lines are also plotted in Gy values.

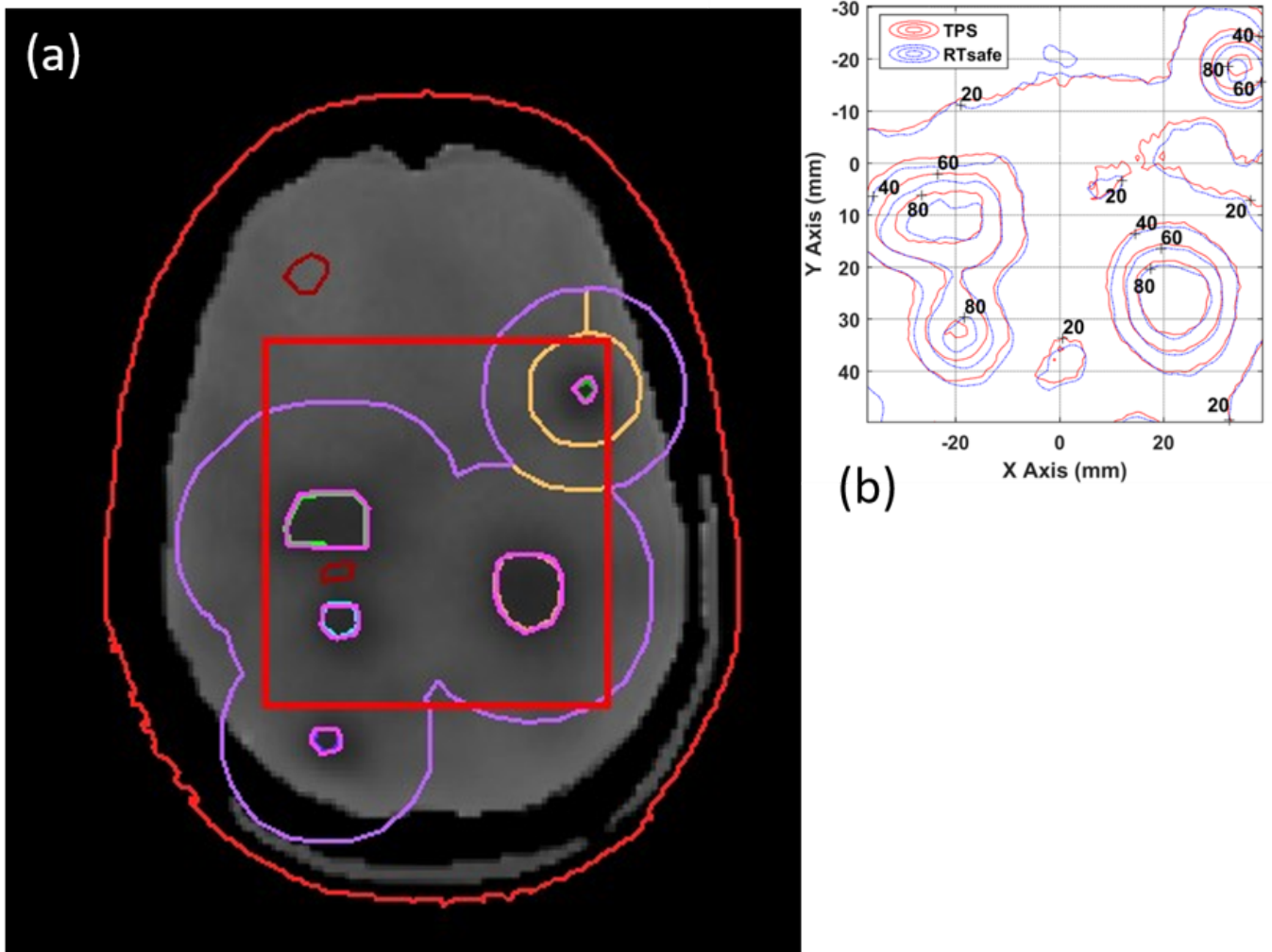


Figure 4

(a) Axial CT image of the real patient with a region of interest. (b) Isodose lines (percentages relative to prescription dose) in the region of interest shown in (a).

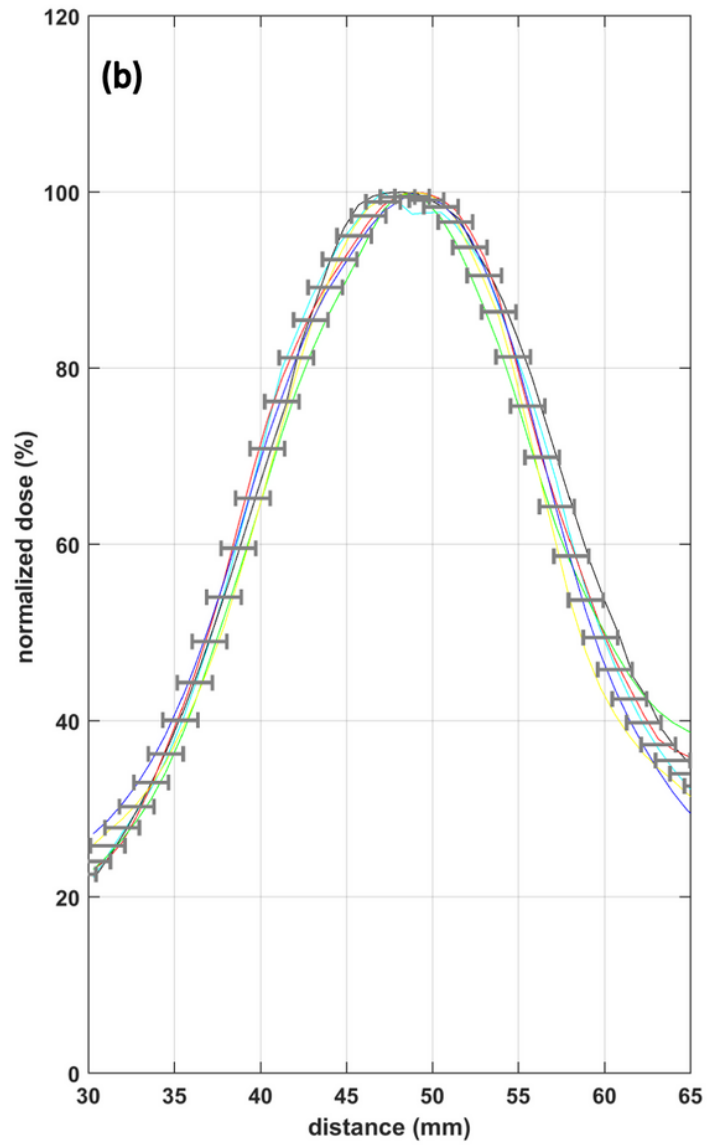
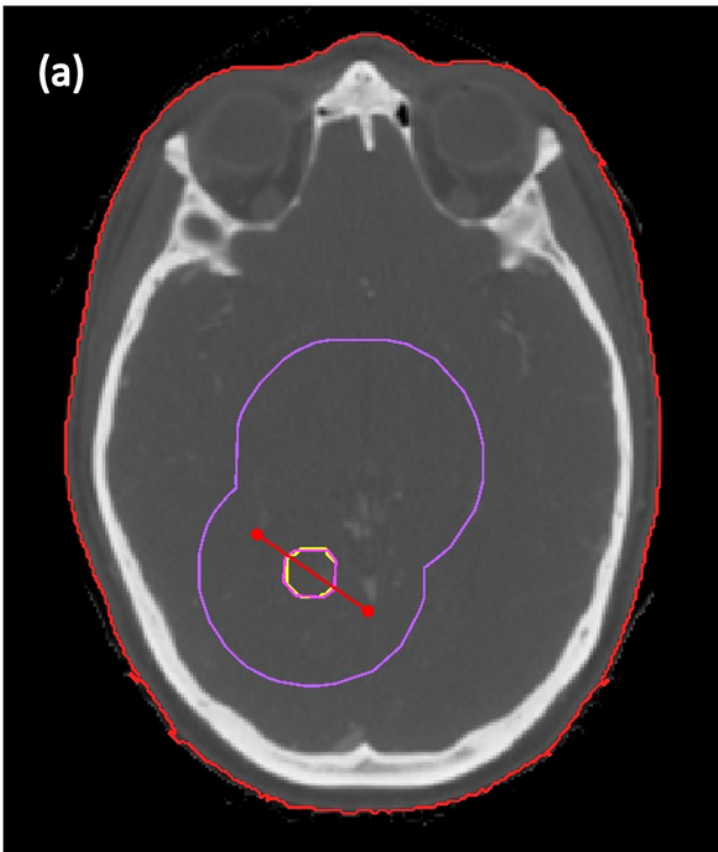


Figure 5

(a) Axial CT image of the real patient. (b) 1D profile comparison between all consortium sites with HexaPOD of measured gel dose distributions (RTsafe) at the location depicted by the red line in (a). Error bars correspond to ± 1 mm spatial uncertainty.

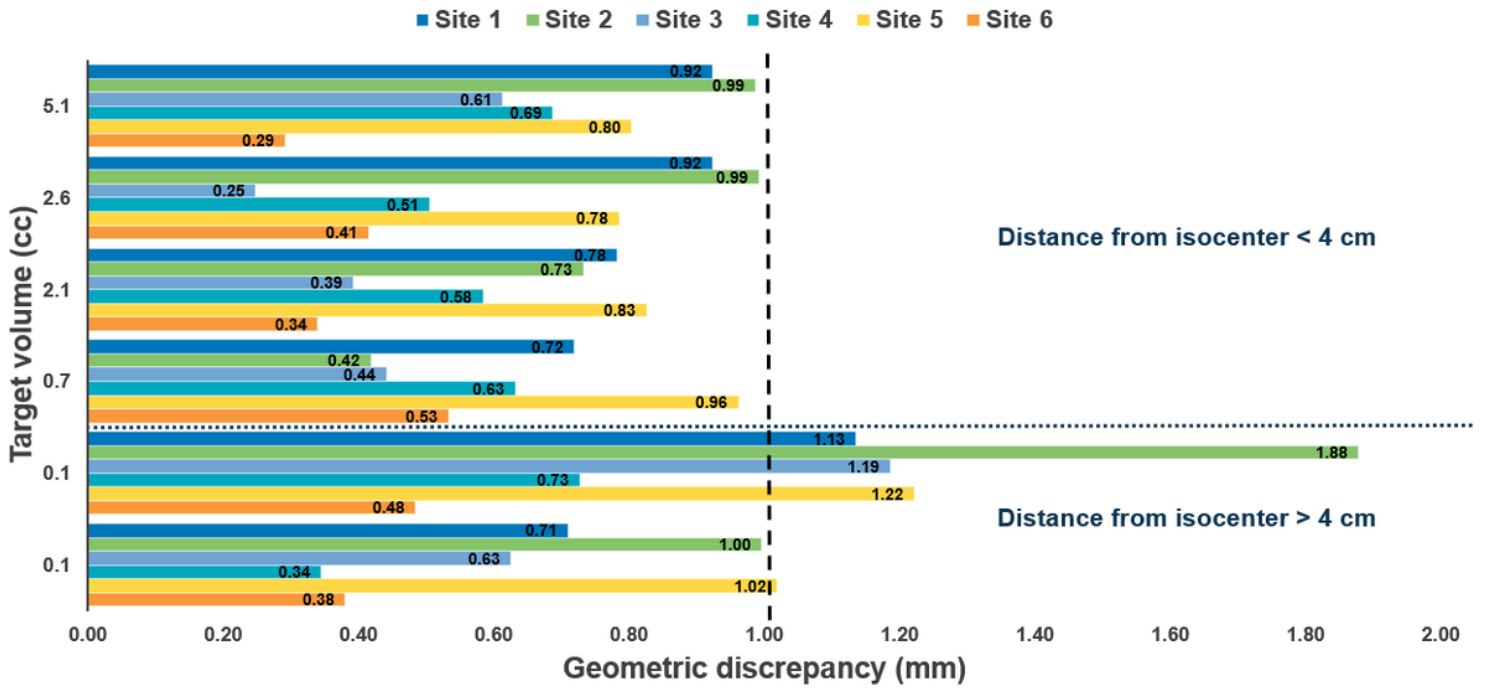


Figure 6

Positional discrepancies between measurement and calculation based on dose distribution center of mass.

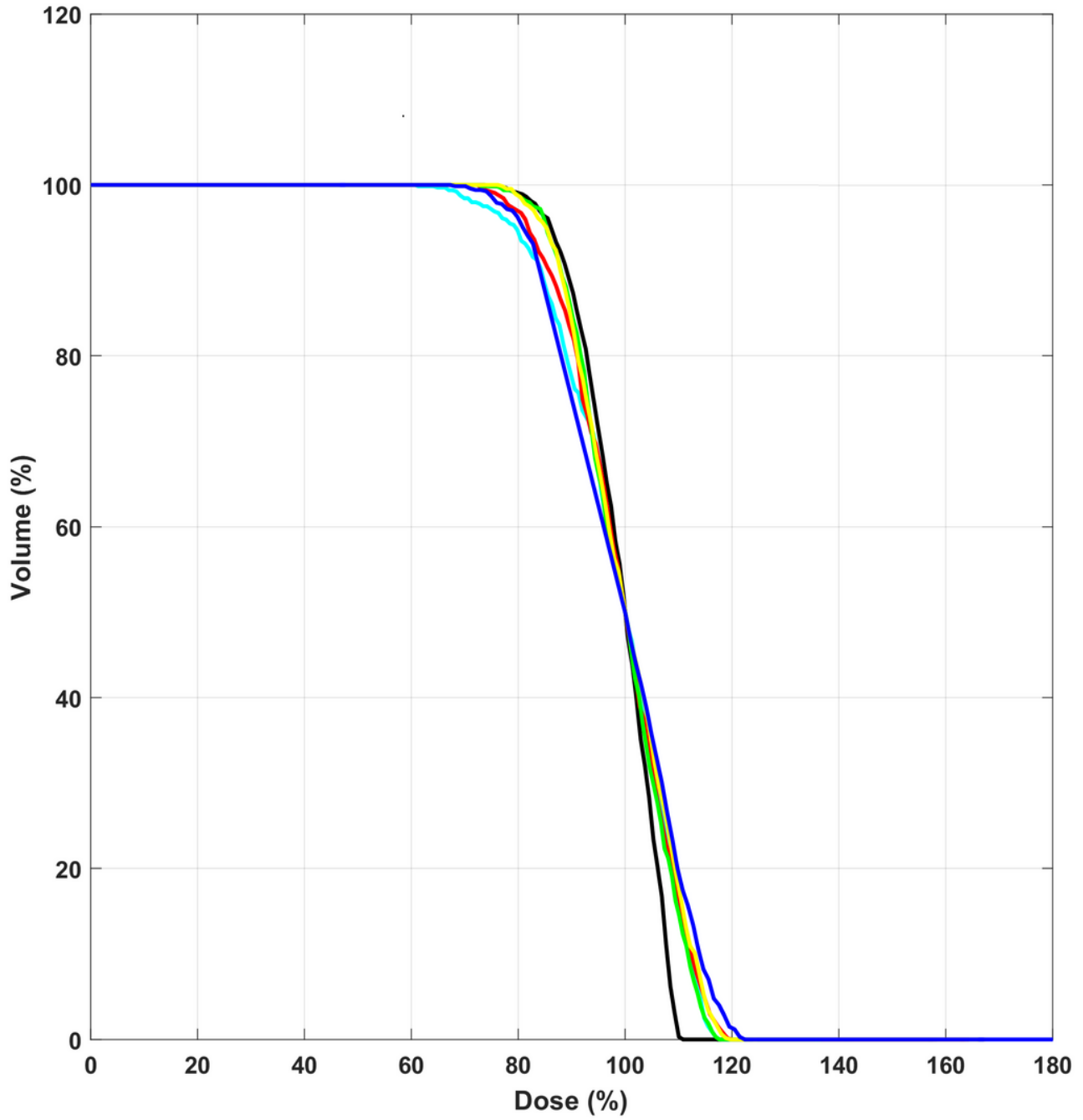


Figure 7

Experimentally measured DVHs from 3D gel data for all six institutions using a HexaPOD tabletop.